Appendix E

If it ain't broke, then what? Taphonomic filters of late Pleistocene Terrestrial Gastropod fossils in the Upper Mississippi Valley

Abstract

This chapter analyzes terrestrial gastropod shell breakage patterns in late Pliestocene sediments from the Upper Mississippi River Valley in order to characterize potential taphonomic biases within four different sedimentary facies. Taxon abundance within each sample was compared to the proportion of those shells that represent broken individuals. These preliminary results show that taphonomic biases were related to shell morphology: tall, narrow shells were the most vulnerable, while some taxa did not show any significant difference in breakage patterns.

Introduction

Late Pleistocene gastropod assemblages from the Upper Mississippi Valley (UMV) present an underutilized proxy record to characterize the regional climate. However, the taphonomic modification of these assemblages must be understood before any ecological interpretation can be made. It is widely recognized that fossil taxa are recovered in unequal proportions. These proportions reflect taphonomic modification of ecological abundance patterns. Much work has been done to characterize the taphonomy of marine shelly deposits (e.g. Flessa et al., 1993), however the influences on continental mollusks remain understudied (Goodfriend, 1992). Previous work on continental mollusk taphonomy is often geared towards recognizing autochthonous versus allocthonous fossil assemblages (La Rocque, 1970; Miller and Bajc, 1990).

The goal of this appendix is to present the prelimary findings of abundance patterns related to the proportion of broken gastropod shells for late Pleistocene fossil

taxa from the UMV. I will describe the influence of factors such as abundance, depositional energy, and morphology upon the proportion of broken individuals in samples of late Pleistocene sediment

Methods

I used the PAST software program (Hammer et al., 2001) to analyze the relationship between facies type and frequency of broken individuals using one-way ANOVAs. I used box plots to represent the central tendencies of the data graphically using box plots. Pearson correlation coefficients were calculated for abundance and broken frequencies using the web-based "Free Statistics Software" interface of Wessa (2008). I excluded singletons from the analysis to avoid overrepresentation of individual shells either whole or broken.

Results

Dataset Overview

The results are summarized in Tables 1-3. The six sites (Figure E1) represent four different depositional facies and radiocarbon results indicate most sites are late full-glacial in age (ca. 16,000 RCYBP), while Limery Coulee dates to the middle late-glacial (ca. 13,400 RCYBP) (Table E1). The 43 samples, weighing a total of 182.4 kg, yielded a total of 12,983 individuals (Table E2). Succineids were the dominant group, accounting for roughly 51% of all specimens recovered. Four genera, *Columella, Vertigo, Pupilla,* and *Discus* were also abundant, representing nearly 49% of the remaining fraction. The

remaining genera were absent at most sites, occurring within a small number of samples (Table E3).

The sites are grouped into four facies associations with varying proportions of coarse-grained sediment. The trough cross-bedded facies is and tabular cross-bedded sand, fine-grained facies colluvium, and fine-grainealluvial silt. The greatest number of samples came from colluvium (n=16), while both alluvial silt and tabular cross-bedded sand were the least sampled (n=7; Table E2). Shell abundance, however, was highest in trough cross-bedded sand facies (n=6,772) and lowest in alluvial silt facies (n=572).

Variation in facies grainsize

Grain size significantly varied (P=0.00001477; Figure E2). Samples from the trough cross-bedded sand facies had the highest median weight percent residuum followed by tabular cross-bedded sands, then colluvium, and alluvial silt, with the least residuum weight percent. The variability of sample residuum weight percent also decreases, with trough cross-bedded facies being the most variable in residuum weight percent and alluvial silt are the least.

Variation in taxon breakage The proportion of broken individuals between all four facies per sample significantly varied for *Columella* (P=0.0001518; Figure E3). In addition, the variability (e.g. intraquartile range) of samples within facies increased as depositional energy decreased. Similarly, the proportion of broken shells varied significantly for *Pupilla* (P=0.01103; Figure E4) when the comparison occurs between the higher energy and lower energy depositional facies, but decreased when all four

facies were analyzed separately (P=0.07239). Samples from high-energy depositional settings that contained shells of *Discus* display no significant variation (P=0.4662; Figure E5). The pattern of increasing variability in lower energy facies seen in *Columella* and *Pupilla* may be present, but only two samples of alluvial silt contained *Discus* shells. In addition, the small sample size likely contributes to the lowered statistical significance. Additional work may be necessary to determine if the weak statistical significance is due to low numbers of specimens, or other factors. Specimens of *Vertigo* showed no variability between facies (P=0.9146) both with median or range.

Discussion

Depositional Energy

It is possible to characterize the potential depositional energy of each facies by using the proportion of residuum. Samples with a larger fraction of coarse (>0.425 mm) material correspond to greater energy required for sediment transport (Figure E1). The highest median values of trough cross-bedded samples represent high depositional energy while alluvial silts represent low depositional energy.

Shell breakage patterns

I interpret the pattern of breakage, visible in three of the most common taxa, of decreasing variability between samples as residuum weight increases as the effect of increased reworking of shells as depositional energy increases. The likelihood of shell breakage increases with the energy of the deposition and transport mechanism, which would also increase proportion of broken individuals incorporated into the fossil

assemblage. While the trend itself is unsurprising, it is important to note that it is not expressed equally among all taxa.

The proportion of broken individuals of both *Pupilla* and *Columella* significantly varied between facies, while *Discus* and *Vertigo* did not (Figures E2-E6). Sparks (1964) noted the vulnerability of *Columella* shells, but suggested that *Pupilla* much more robust. He noted that, although the shell is rather thin, the ratio of its height to its width is relatively low, making breakage due to asymmetric stress on the shell less likely. Similarly, Briggs et al. (1990) also noted few broken *Pupilla* shells in braided stream habitats in the Austrian Alps. Carter (1990) found that there was differential preservation in the aperture of *Pupilla* in temperate, humid soils. The results of this study suggest that *Pupilla* is among the more vulnerable of taxa, however whether the shells are broken as a result of external influences such as soil moisture or depositional energy or related to shell structure is not known. *Pupilla* is often associated with xeric, open habitats (Pilsbry, 1948; Leonard, 1952), which may be located further away from active floodplains where trough and tabular cross-bedded sands are deposited. Shells of *Pupilla* may be transported further distances relative to other taxa.

Shells of *Discus* weakly follow the pattern of increased variability in broken proportions with decreased depositional energy (Figure E5). Sparks (1964) noted that relatively small, discoidal shells were most often broken as a result of sediment compaction. It is unlikely that sediment compaction affects *Discus* breakage in the trough cross-bedded facies, since coarser sediments do not compact as much as finer sediments. The lack of *Discus* shells may be a result of ecological factors that limit its abundance in areas of alluvial silt deposition.

It is interesting to note that *Vertigo* does not display any significant variation in the number of broken individuals per sample between facies (Figure E6). Sparks (1964) mentioned this genus was relatively resistant to breakage because of its shape. Shells of *Vertigo* are relatively small and oval in shape, which may provide some resistance to breakage. It may also be that *Vertigo* may not pass through similar taphonomic "filtering" as compared to other pupillids such as *Columella* and *Pupilla* (c.f. Behrensmeyer et al. 2000), or that the process of shell breakage is more random. Alternatively, it may be that Vertigo shells were transported relatively short distances due to the fact they inhabited areas of deposition for all four sampled facies.

Rare genera such as *Vallonia* and *Euconulus* were obtained as mostly and entirely complete shells, respectively (Table E3). *Hendersonia*, however, is represented by exclusively broken shells. It may be that the threshold for detecting fragments of *Vallonia* and *Euconulus* is high. One needs nearly whole shells to retain sufficient shell characters for identification. Hendersonia, however, has a very unique shell with thick, flattened whorls and a distinct apertural callus that remain identifiable even with very small (ca. 2mm) fragments. Rare species with morphologically indistinct shells may be hard to detect as broken fragments, while distinct shells, such as Hendersonia, will be easy to recover.

Hendersonia may also represent a unique taphonomic pathway. Its shell is relatively large, especially compared to other full-glacial gastropods and may occur as exclusively broken fragments as the result of selective predation or as a result of reworked, older material. An amino acid racemization analysis of these fragments is planned for the summer of 2009.

The abundance of succineid gastropods may represent the supply-side influence of taphonomy (e.g. reproduction rate) or reflect high local abundance in a wide variety of depositional settings (c.f. Frest and Dickson, 1986). Succineid gastropods produce far more individual shells than any other taxa. Detailed analysis of this possibility is beyond the scope of this study, but it may be related to the reproductive mode of gastropod taxa. There is some evidence to suggest that many succineids reproduce semelparously, whereas most other species are iteroparous (Pilsbry, 1948). Semelparous species will tend to produce fewer shells per generation; while iterparous species will produce many offspring once and then die, adding more dead shells compared to iteroparous taxa.

Conclusions

The results from this study show that the highest proportion of broken individuals occurred within samples from high-energy trough cross-bedded and tabular cross-bedded sand facies as compared to samples from the lower energy colluvium and alluvial silt facies (e.g. *Columella* Figure 3). The range of values was also lower in higher energy facies compared to the lower energy facies. This trend likely reflects the increased probability that higher energy depositional mechanisms will break the shell. The higher proportion of broken individuals in higher energy facies is a result of more broken individuals, while the narrower range could be due to a closer balance between input of whole shells and their subsequent destruction.

Site	Facies	^{14}C Age	Lab Number	No. Samples
Kulas Quarry (KQ)	TAB/TRO	17,550±70 16,670±60	Beta-	20
Hwy-JJ (JJ)	COLL	16,120±60	Beta-	6
Big Platte (BP)	COLL	15,710±50 15,890±50 15,800±100	Beta-	8
Storer Creek (SC)	SILT	15,800±50	Beta-	5
Root River (RR)	SILT	15,983±136*	*	2
Limery Coulee (LC)	COLL	13,430±70 13,460±50	Beta-	2

Tab = Tabular Cross-Bedded Sand, Tro = Trough Cross-Bedded Sand, COLL = Colluvium, SILT = Alluvial Silt

*Age data from Mason and Knox (1997)

Table E1. Sedimentary facies, radiocarbon age, and number of samples obtained from sites discussed in text. Date for Kulas Quarry represents an upper section and lower section date, while remaining dates obtained from base of site exposures.

Facies	No. Samples	Total Weight (Kg)	Total No. Shells
Trough Cross-Bedded Sand	13 (30.2%)	56.25 (30.8%)	6,772 (52.1%)
Tabular Cross-Bedded Sand	7 (16.3%)	24.61 (13.5%)	2,038 (15.7%)
Colluvium	16 (37.2%)	75.84 (41.6%)	3,601 (27.7)
Alluvial Silt	7 (16.3%)	25.70 (14.1%)	572 (4.4%)
Total	43	182.41	12,983

Table E2. Number of samples, weight, and total number of individual shells obtained from the four sedimentary facies discussed in the text.

Taxon	Tot Shells (% Broken)	Sites						
		KQ-TRO	KQ-TAB	JJ	BP	RR	SC	LC
Succinidae*	6726 (6.6%)	3991 (7.4%)	1158 (18.4%)	298 (9.7%)	813 (1.4%)	102 (4.9%)	250 (7.6%)	99 (1%)
Vertigo	2028 (25.8%)	929 (25.9%)	283 (25.4%)	79 (22.8%)	631 (18.2%)	66 (19.7%)	52 (23.1%)	265 (16.2%)
Columella	1886 (73.8%)	999 (84.7%)	284 (81.3%)	46 (65.2%)	373 (50.1%)	49 (51%)	15 (33.3%)	120 (56.7%)
Discus	1807 (16.3%)	633 (19.7%)	228 (14%)	29 (24.1%)	517 (13.9%)	16 (6.3%)	1 (0%)	383 (15.1%)
Pupilla	669 (77.1%)	200 (89%)	79 (82.3%)	104 (78.8%)	95 (49.5%)	14 (85.7%)	7 (42.9%)	169 (75.7%)
Vallonia	179 (6.1%)	-	-	-	28 (21.4%)	-	-	151 (3.3%)
Hendersonia	27 (100%)	20 (100%)	6 (100%)	-	-	-	-	1 (100%)
Euconulus	11 (0%)	-	-	-	8 (0%)	-	-	3 (0%)
Total Shells	12983	6772	2038	556	2465	247	325	1191
r^2	0.0165	0.2851	0.1163	0.0915	0.0007	0.2772	0.1669	0.1096
P (1-sided)	0.3534	0.08645	0.2042	0.28002	0.4276	0.18104	0.2474	0.17503

*Four samples (three from KQ-TRO and one from KQ-TAB) were not used to calculate broken percentage due to high (>1000) abundance of succineid shells. Counting was also halted at 1000 individuals for each sample.

r^2 and *P* values calculated via Pearson Correlation of taxon frequency abundance and broken proportion

Table E3. Summary table of all taxon abundance and proportion of broken individuals at each site discussed in the text. Kulas Quarry split into two separate facies. P and r2 values calculated via pearson correlation of taxon frequency abundance and proportion of broken individuals.

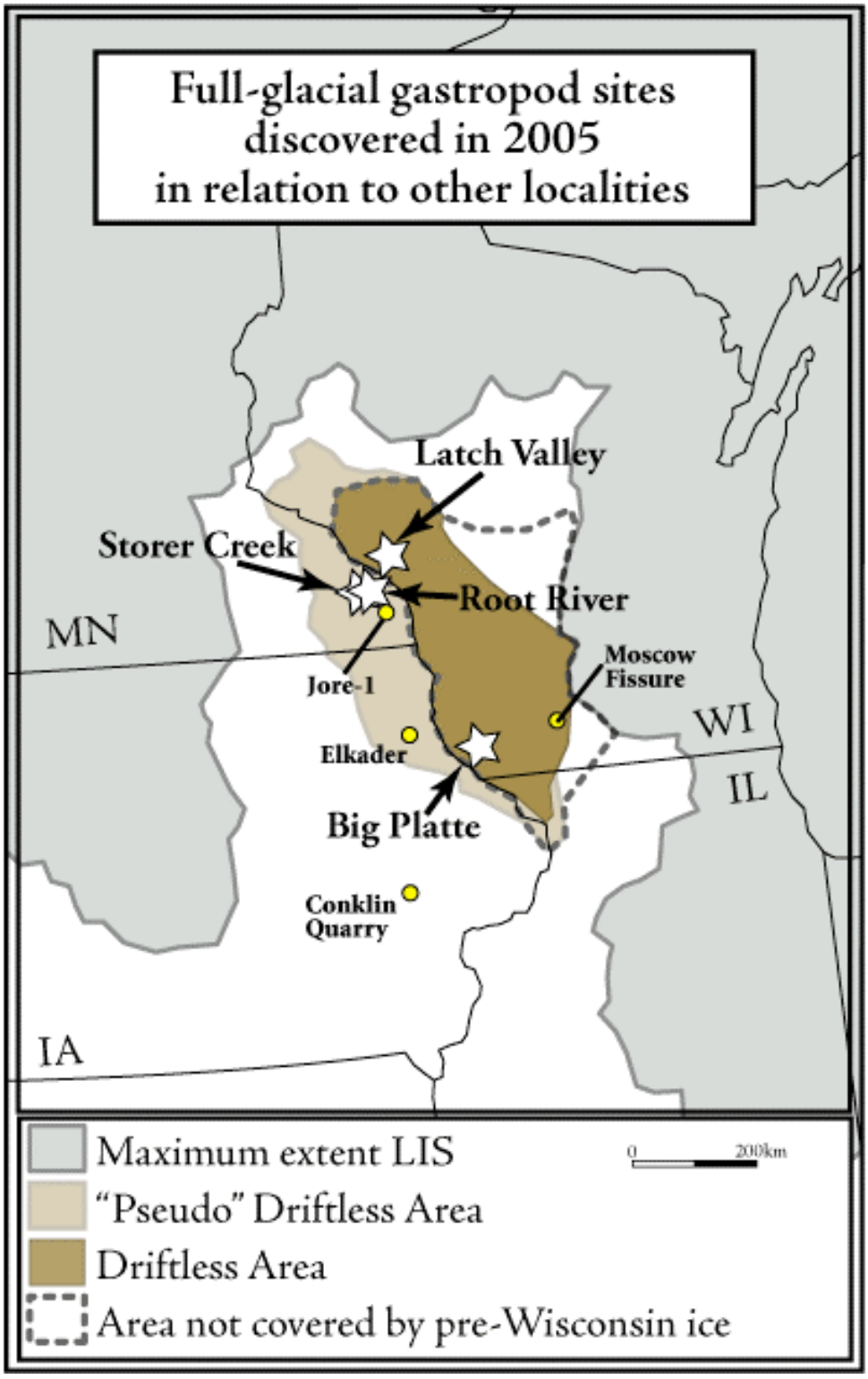

Figure E1. Field sites referred to in Appendix D.

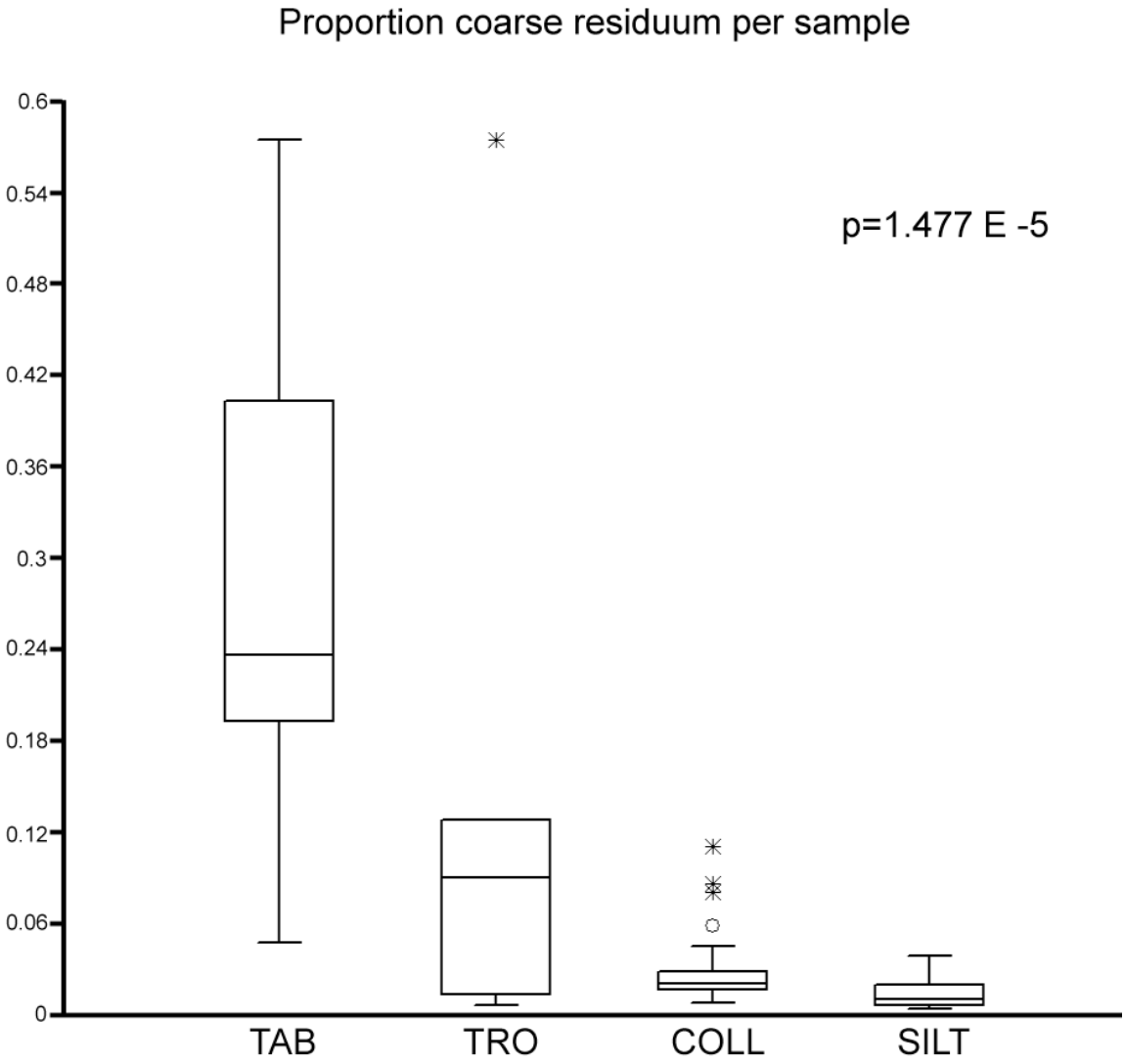

Figure E2. Box plot showing proportion of residuum per sample from all four facies discussed in text. P value calculated via one-way ANOVA.

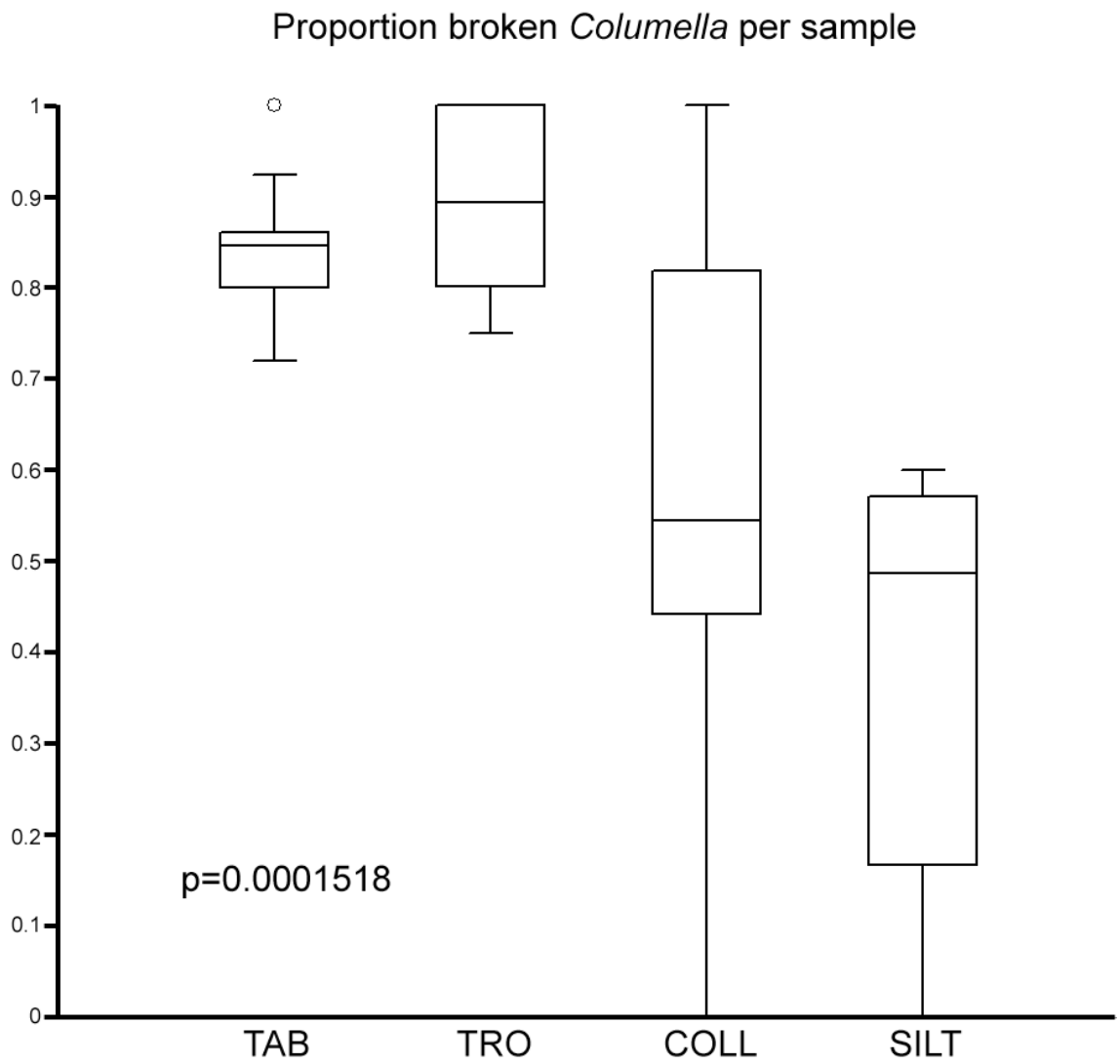

Figure E3. Box plot showing the proportion of broken *Columella* per sample within depositional facies. P value calculated via one-way ANOVA.

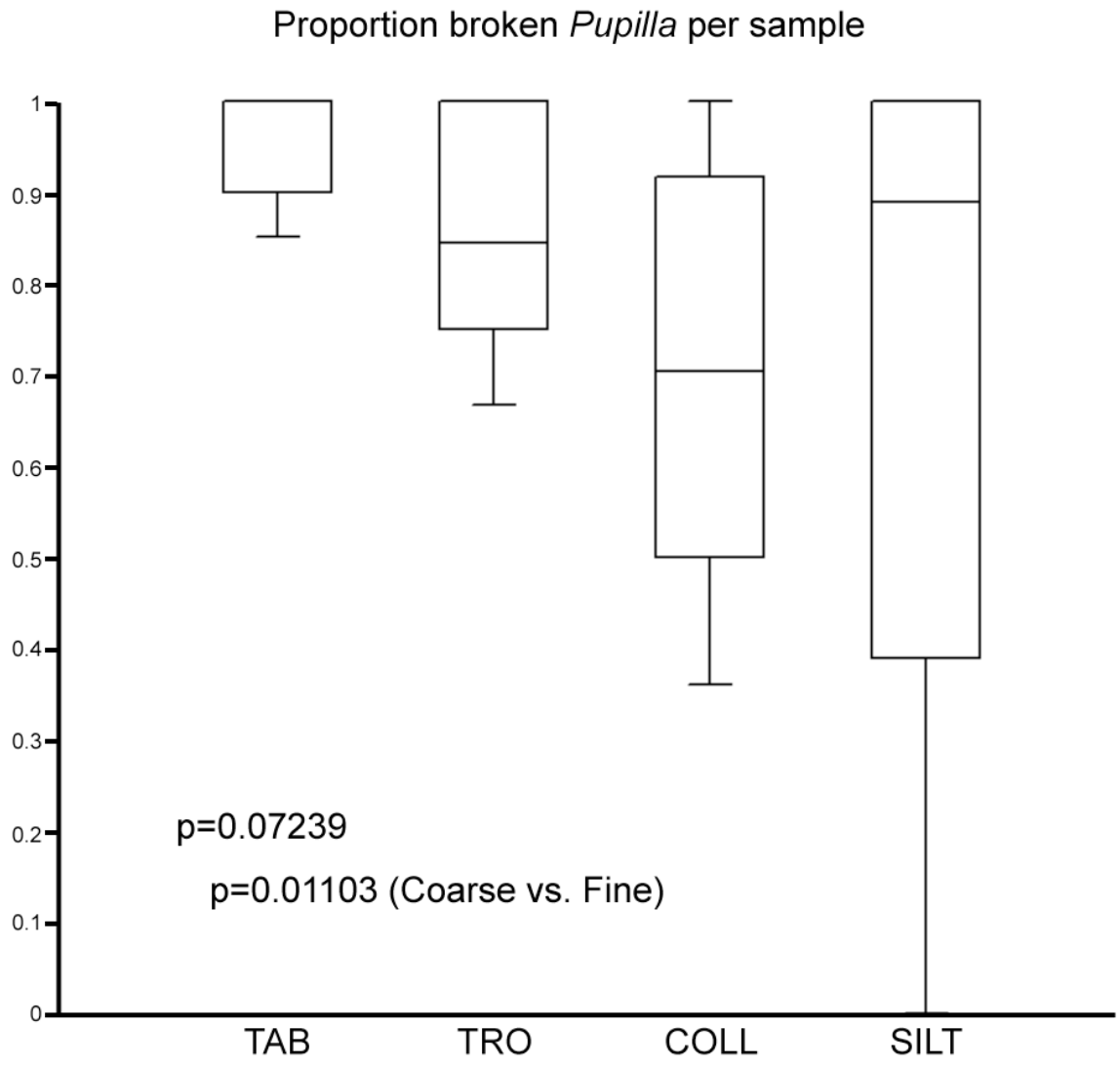

Figure E4. Proportion of broken Pupilla shells per sample from all four facies discussed in text. P values calculated from one-way ANOVA.

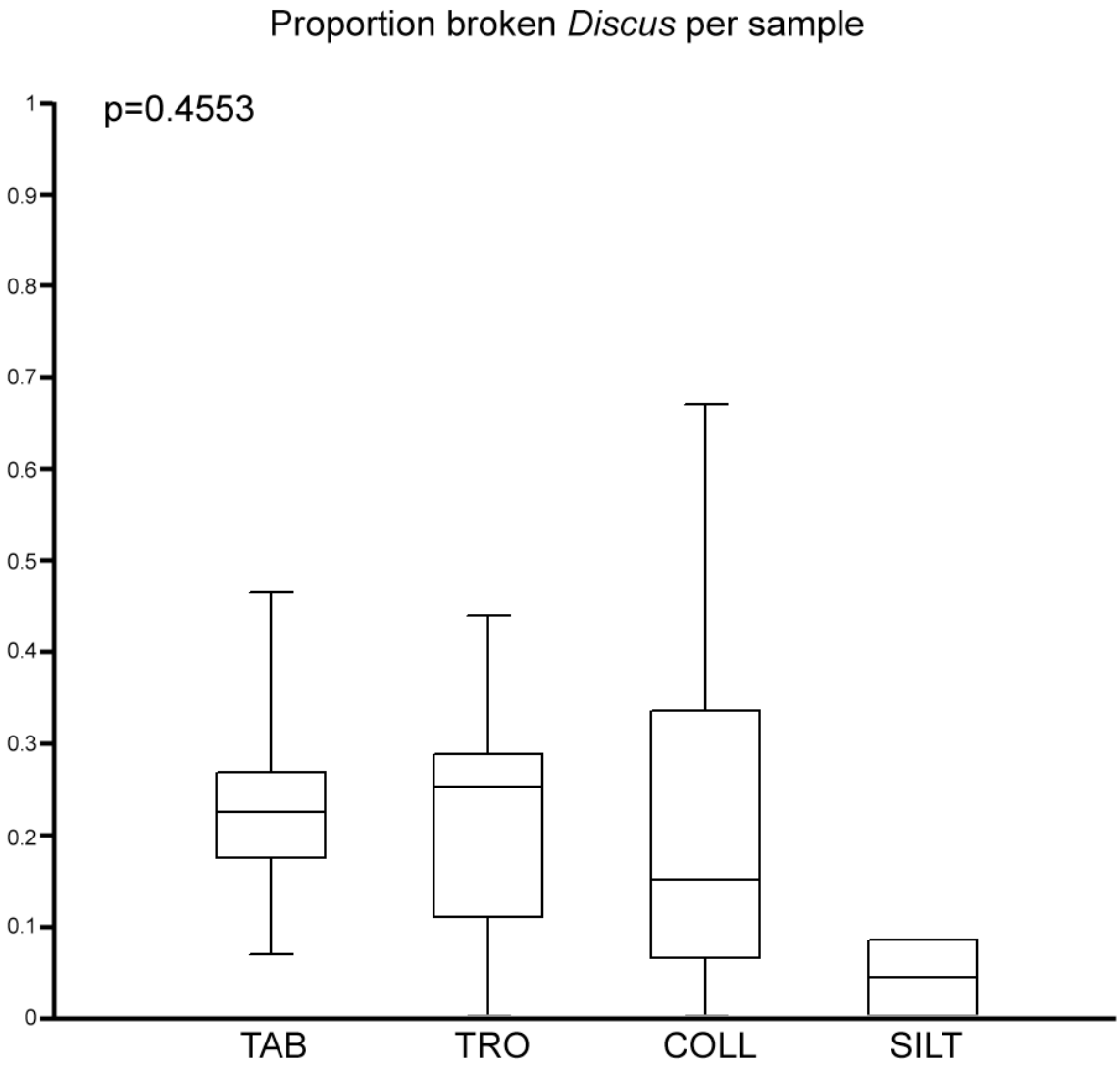

Figure E5. Proportion of *Discus* shells broken per sample among each facies. P value calculated via one-way ANOVA.

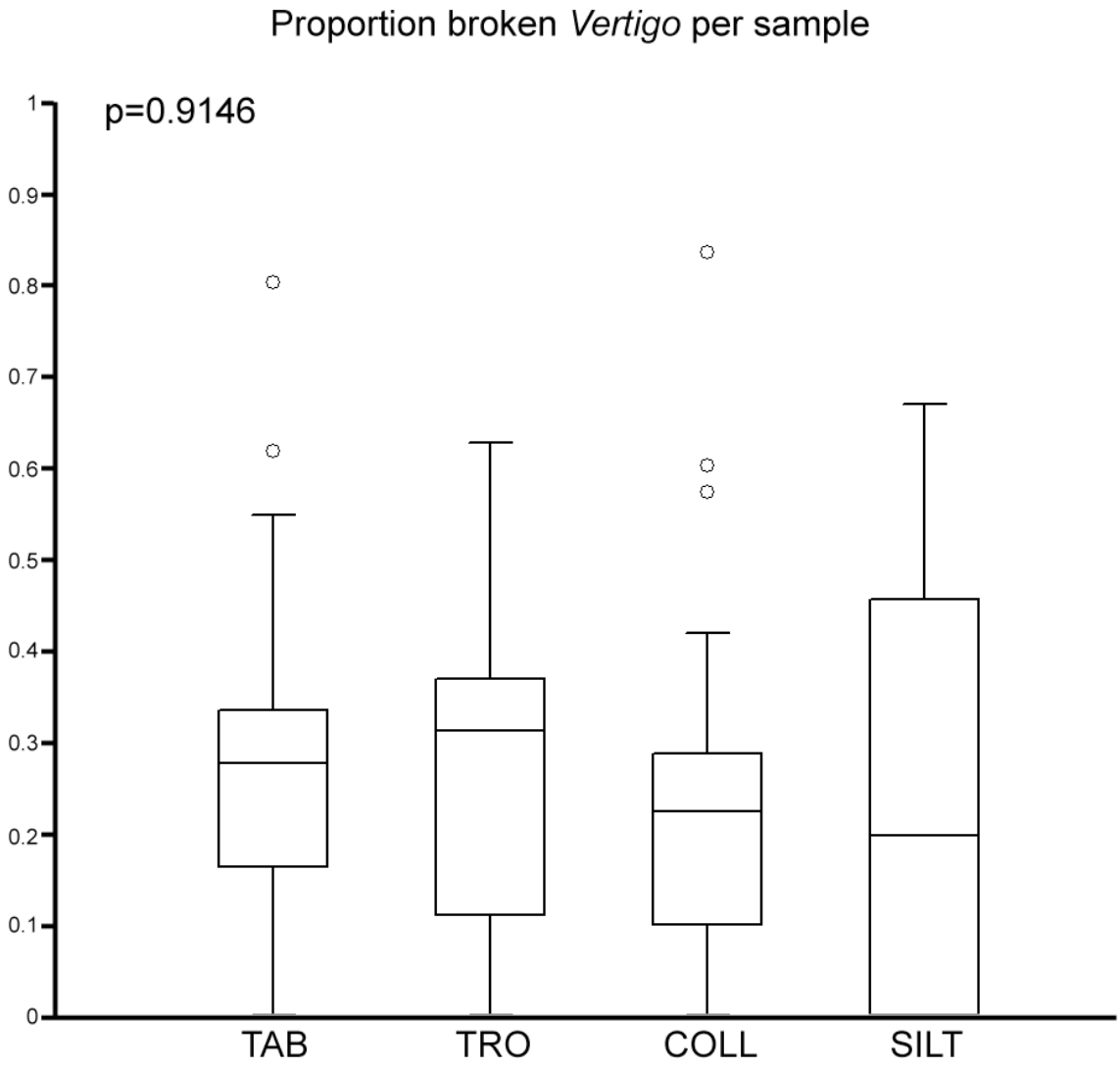

Figure E6. Proportion of *Vertigo* shells broken per sample among each facies. P value calculated via one-way ANOVA.